Ecological Indicators 80 (2017) 84–95

Contents lists available at ScienceDirect

Ecological Indicators

journal homepage: www.elsevier.com/locate/ecolind

Original Articles

Satellite monitoring of cyanobacterial harmful algal bloom frequency in recreational waters and drinking water sources

John M. Clark[a], Blake A. Schaeffer[b,*], John A. Darling[b], Erin A. Urquhart[a], John M. Johnston[b], Amber R. Ignatius[a], Mark H. Myer[a], Keith A. Loftin[c], P. Jeremy Werdell[d], Richard P. Stumpf[e]

[a] ORISE Fellow, U.S. Environmental Protection Agency, Office of Research and Development, National Exposure Research Laboratory, USA
[b] U.S. Environmental Protection Agency, Office of Research and Development, National Exposure Research Laboratory, USA
[c] U.S. Geological Survey, Kansas Water Science Center, Lawrence, KS, USA
[d] Ocean Ecology Laboratory, NASA Goddard Space Flight Center, Greenbelt, MD, USA
[e] National Oceanic and Atmospheric Administration, National Centers for Coastal Ocean Science, Silver Spring, MD, USA

ARTICLE INFO

Keywords:
Cyanobacteria
Drinking water
Recreational water
Satellite
Public water systems
Harmful algal blooms

ABSTRACT

Cyanobacterial harmful algal blooms (cyanoHAB) cause extensive problems in lakes worldwide, including human and ecological health risks, anoxia and fish kills, and taste and odor problems. CyanoHABs are a particular concern in both recreational waters and drinking water sources because of their dense biomass and the risk of exposure to toxins. Successful cyanoHAB assessment using satellites may provide an indicator for human and ecological health protection. In this study, methods were developed to assess the utility of satellite technology for detecting cyanoHAB frequency of occurrence at locations of potential management interest. The European Space Agency's MEdium Resolution Imaging Spectrometer (MERIS) was evaluated to prepare for the equivalent series of Sentinel-3 Ocean and Land Colour Imagers (OLCI) launched in 2016 as part of the Copernicus program. Based on the 2012 National Lakes Assessment site evaluation guidelines and National Hydrography Dataset, the continental United States contains 275,897 lakes and reservoirs > 1 ha in area. Results from this study show that 5.6% of waterbodies were resolvable by satellites with 300 m single-pixel resolution and 0.7% of waterbodies were resolvable when a three by three pixel (3 × 3-pixel) array was applied based on minimum Euclidian distance from shore. Satellite data were spatially joined to U.S. public water surface intake (PWSI) locations, where single-pixel resolution resolved 57% of the PWSI locations and a 3 × 3-pixel array resolved 33% of the PWSI locations. Recreational and drinking water sources in Florida and Ohio were ranked from 2008 through 2011 by cyanoHAB frequency above the World Health Organization's (WHO) high threshold for risk of 100,000 cells mL^{-1}. The ranking identified waterbodies with values above the WHO high threshold, where Lake Apopka, FL (99.1%) and Grand Lake St. Marys, OH (83%) had the highest observed bloom frequencies per region. The method presented here may indicate locations with high exposure to cyanoHABs and therefore can be used to assist in prioritizing management resources and actions for recreational and drinking water sources.

1. Introduction

Harmful algal blooms are environmental events that occur when algal populations achieve sufficiently high density resulting in negative environmental or health consequences (Smayda, 1997). Blooms associated with photosynthetic prokaryotes (cyanobacterial harmful algal blooms [cyanoHAB]) occur worldwide and have been documented across the United States (Loftin et al., 2016). Toxic blooms are a global issue and examples exist on every continent such as the Baltic Sea in Europe (Kahru et al., 2007), Lake Victoria in Africa (Verschuren et al., 2002), Lake Taihu in Asia (Duan et al., 2009), Lake Erie in North America (Stumpf et al., 2012), Murray River in Australia (Al-Tebrineh et al., 2012), several reservoirs in South America (Dörra et al., 2010), and even Antarctica (Hitzfeld et al., 2000). Harke et al. (2016) reported documented events of the freshwater *Microcystis* species in 108 out of 257 countries and territories. Many U.S. states have issued health advisories or closed recreational areas due to potential risks from cyanoHAB exposure (Chorus, 2012; Graham et al., 2009). CyanoHABs typically result from a combination of excess nutrients (Michalak et al., 2013) and other environmental conditions, such as warming tempera-

* Corresponding author.
E-mail address: schaeffer.blake@epa.gov (B.A. Schaeffer).

http://dx.doi.org/10.1016/j.ecolind.2017.04.046
Received 8 November 2016; Received in revised form 17 April 2017; Accepted 18 April 2017

tures and water column stratification (Paerl and Huisman, 2008). Alterations in land-use practices, such as urbanization or agricultural practices, can change sediment loading and increase nutrient delivery in watersheds (Lunetta et al., 2010), which is known to influence cyanobacterial growth. CyanoHABs can produce an array of potential toxins and cause nuisance odors, hypoxia, and unappealing surface scums creating a potential for adverse recreational exposure and ecological impact (Codd et al., 2005a). Additional consequences of cyanoHABs may include undesirable finished drinking water, increased drinking water treatment costs, and economic and infrastructure costs such as loss of revenue from recreational systems and from businesses that rely on potable water (Dodds et al., 2009; Steffensen, 2008).

Water quality is a critical consideration in determining water resource availability for human consumption, aquatic life, and recreation (U.S. EPA, 2013b). Despite sufficient water quantity, water availability may be limited if quality does not meet the requirements of intended use. CyanoHAB toxins frequently limit water resource availability by negatively impacting water quality and rendering it unsuitable for multiple uses. Potential short- and long-term human health effects of cyanoHABs and the toxins they produce include dermatitis; gastrointestinal, respiratory, and neurological impairments; and adverse impacts to liver and kidney function. These effects may reduce the availability of drinking water resources and increase treatment costs (Hilborn et al., 2014). CyanoHABs and associated toxins have been identified in drinking water sources throughout the world (Hoeger et al., 2005). Documented events include impaired drinking water resources at Haimen city, Fusui county, China, in 1993 and 1994 (Ueno et al., 1996); Wuxi city, Jiangsu, China in May 2007 (Qin et al., 2010); Caruaru, Brazil, in 1996; and Australia in 1983 (Falconer and Humpage, 2005). Depending on the severity of a cyanoHAB event, municipalities may issue “Do Not Drink” advisories, as they did in Carroll Township, Ohio, in September 2013 (Henry, 2013) and in Toledo, Ohio, in August 2014 (Sonich-Mullin, 2014).

An additional route of cyanoHAB toxin exposure is through recreational contact, including dermal and oral contact, with occasional exposure through inhalation of surface waters (Backer et al., 2015; Backer et al., 2010; Codd et al., 2005b). Adverse human health impacts from recreational exposure to cyanoHABs include, but are not limited to, headaches and allergic reactions, including blistering, vomiting, and diarrhea (Falconer, 1999; Stewart et al., 2006b). CyanoHABs also pose risks to non-human populations. Negative impacts include canine illness and death, where the number of reported events and animals affected has increased over the past 50 years (Backer et al., 2013). Wildlife and livestock illness and death have been globally reported in animals ranging from traditional farm stock to fish, birds, and insects (Backer et al., 2015; Hilborn and Beasley, 2015). In birds, cyanobacterial toxins can cause neurological disease leading to brain lesions and death. The documented deaths of over 170 bald eagles, thousands of American coots, the federally endangered Florida snail kite, and other species of wild birds have been caused by cyanoHAB events (Dodd et al., 2016).

Cell counts and microcystin concentrations are most commonly used to evaluate potential human health risk, and many states have customized thresholds based on additional information gathered locally (Graham et al., 2009). The World Health Organization (WHO) has a three-level guideline approach, which describes concentrations of the ubiquitous photosynthetic pigment chlorophyll-a and cyanobacterial cell abundance (cells/mL) to determine the level of associated risk to support a warning or closure. WHO provides estimates of microcystin that could correspond to the cell abundance at each guideline level. The U.S. Environmental Protection Agency (U.S. EPA) also has the drinking water health advisory for cyanobacteria microcystins toxin (U.S. EPA, 2015a).

Many U.S. states have experienced challenges in developing monitoring programs for cyanoHABs because of the need to cover large geographic areas with insufficient resources. The presence of cyanotoxins is a primary indicator of human health risk, but quantifying all forms and derivatives of the related toxins is difficult, expensive, and time-intensive. There are approximately 246 variants of microcystin-LR, 3 variants of cylindrospermopsin, and 7 variants of anatoxins (Loftin et al., 2016; Meriluoto et al., 2017; U.S. EPA, 2014). Loftin et al. (2016) highlights that WHO thresholds agreed in only 27% of cases between all three recreational risk metrics (cyanobacteria abundance, chlorophyll-*a*, and microcystins) when applied against the 2007 National Lakes Data (2007 NLA), clearly demonstrating that the presence of chlorophyll-*a* does not always equate to cyanoHABs and that cyanobacterial abundance can result in over-prediction of microcystin recreational risk. However, microcystin may not be a good predictor of other classes of toxins also produced by cyanoHABs with co-occurrence between cylindrospermopsins, microcystins, and saxitoxins only 0.32% of 2007 NLA samples. Epidemiological studies have reported statistically significant associations between inflammatory and allergenic human health exposure to water containing cyanoHAB cells (Lévesque et al., 2016; Lévesque et al., 2014; Lin et al., 2016; Pilotto et al., 1997). Some adverse health endpoints may not be associated with exposure to known toxins (Stewart et al., 2006a; Stewart et al., 2006b). Thus cyanobacterial abundance is perhaps better suited for assessing nationwide risks depending on the balance between public health and socioeconomics. In consideration of these challenges and uncertainties, new tools and methods are needed to help develop reliable and cost-effective monitoring programs at lake, watershed, state, regional, and national scales with sufficient spatial-temporal resolution to detect change where field monitoring alone may not provide sufficient coverage.

This study explores the possibility of using satellite remote sensing technology to assess cyanoHAB abundance for spatially resolvable inland recreational and public water supply lakes, reservoirs, and ponds using algal pigments as surrogates for HAB and cyanoHAB abundance related human health risk thresholds. The presence of cyanoHAB abundance estimated from satellites can be used to prioritize waterbodies requiring further evaluation for cyanotoxins. Although satellite observations cannot detect toxins (Stumpf et al., 2016), they can be used to quantify cyanoHAB abundance (Kutser, 2009). Previous studies provide a comprehensive review of past, present, and new satellite sensors available for deriving water quality in estuaries and inland waters (Dörnhöfer and Oppelt, 2016; Tyler et al., 2016). The advantages and disadvantages of sensor spatial, spectral, temporal resolution, and other parameters are also discussed in other studies (Mouw et al., 2015), along with recent progress updates (Palmer et al., 2015).

The use of satellites for management involves spatial coverage of both recreational and drinking water lakes and reservoirs. Satellite remote sensing has reportedly detected cyanoHAB abundance in drinking water sources, and most efforts to date have focused primarily on algorithm development, validation, and refinement (Medina-Cobo et al., 2014; Song et al., 2013; Song et al., 2014). Satellites can provide a synoptic survey, but their scope of application is poorly defined. Water quality managers need to understand the number of lakes and reservoirs resolvable by satellite. Once the scope of application is defined, it may be possible to use satellite technology to support management needs such as providing occurrence information relevant to the national Safe Drinking Water Act (SDWA) Contaminant Candidate List (CCL) (U.S. EPA, 2013a, 2016a) and the Unregulated Contaminant Monitoring Rule (UCMR) (U.S. EPA, 2016b). The SDWA’s CCL includes drinking water contaminants (such as cyanotoxins) known or anticipated to occur in public water systems not currently subject to regulations. The UCMR includes contaminants suspected to be present in drinking water that do not yet have set standards under the SDWA. Selection of contaminants for the UCMR is largely based on the CCL.

The objectives of this study are to (1) determine the number of surface water bodies on the basis of permissible use as recreational and drinking water sources viewable with existing pixel resolutions (defined as the minimum spatial detection area) measured by satellites licensed

for public use and (2) examine the cyanoHAB frequency above recreational risk thresholds in two U.S. states (Florida and Ohio) on the basis of phycocyanin using four Area of Interest (AOI) categories. AOI categories allowed the frequency of occurrence to be calculated on the same base group of lakes, used in each category (see Section 2.3), and could be compared with water pixels associated with a public water surface intake (PWSI). More broadly, this study explores issues relevant to understanding the general utility of remotely sensed data for cyanoHAB occurrence monitoring including the spatial resolvability of waterbodies based on the pixel resolution of currently operational satellite sensors and those likely to become operational in the near future, the spatio-temporal coverage of satellite data relevant to assessments, and the possibility of developing transferrable methods capable of determining cyanoHAB occurrence at specific points of management interest (such as drinking water intakes and recreational waterbodies).

2. Materials and methods

2.1. Satellite derivation of cyanoHAB abundance

Full resolution (300 m at nadir) scenes from the European Space Agency's MEdium Resolution Imaging Spectrometer (MERIS) were obtained for parts of Florida and Ohio between the years 2008 and 2011 (Fig. 1). Nadir is defined as the point directly below the satellite on the Earth surface. Standard MERIS Level–1B data are archived at the NASA Ocean Color website https://oceandata.sci.gsfc.nasa.gov/. Data were processed using the National Oceanic and Atmospheric Administration's (NOAA) satellite automated processing system, which incorporates the National Aeronautics and Space Administration (NASA) standard ocean color satellite processing software distributed within the NASA Sea-viewing Wide Field-of-view Sensor (SeaWiFS) Data Analysis System (SeaDAS) version 7.1 (Baith et al., 2001) package and the Shuttle Radar Topography Mission (SRTM) GC land mask (Carroll et al., 2009). Images were processed to Universal Transverse Mercator (UTM) projection with nearest-neighbor interpolation. Estimates of spectral surface albedo, Rhos, were generated by removing Rayleigh radiances from the top-of-atmosphere signal measured by the satellite. Clouds were masked using a spectral albedo threshold algorithm that accounts for turbid water to eliminate misidentification of pixels with bright reflectances resulting from intense blooms as clouds. Mixed land-water pixels were identified when Rhos(885) was > both Rhos(709) and Rhos(754). The Rhos estimates were used to calculate the Cyanobacteria Index (CI) from the spectral shape algorithm centered on 681 nanometers (nm), CI = −SS(681) (Wynne et al., 2008), routinely used in Lake Erie (Stumpf et al., 2016). The MERIS CI output for each image then was converted to cyanoHAB abundance in cells per milliliter (cells mL^{-1}) following Wynne et al. (2010), where cyanoHAB abundance = 1.0×10^{8}*CI. Field validation of the CI algorithm (Fig. 2) was previously demonstrated in the same regions as this study (Lunetta et al., 2015; Tomlinson et al., 2016). Weekly 7-day composite images were created by retaining the maximum value detected for each pixel within the time period. The weekly composites were transformed to Albers Equal Area projection with nearest-neighbor interpolation to match the projections of the National Hydrography Dataset (NHD).

2.2. Spatial coverage of water bodies

The ability of a satellite to resolve a waterbody depends on the ideal pixel size of the satellite sensor at nadir and on the combined size and geometry of the waterbody. A waterbody mask was generated using the NHD Plus version 2.0 (NHDPlusV2) (McKay et al., 2012) to identify waterbodies that could be resolved by satellites. All NHDPlusV2 features classified as lakes, ponds, and reservoirs were extracted and then filtered using U.S. EPA's 2012 National Lakes Assessment (NLA) site evaluation guidelines (U.S. EPA, 2011). Waterbodies classified as intermittent or estuarine, or with a surface area < 1 ha, were excluded from further analysis based on NLA criteria. Remaining NHDPlusV2 NLA waterbodies were rasterized at 30 m spatial resolution to match the highest nadir pixel resolution of the multi-spectral bands on operational satellites such as the Landsat 8 Operational Land Imager (OLI) or Sentinel-2 series MultiSpectral Instruments (MSI).

The waterbody spatial coverage with resolvable satellite pixels was calculated based on the minimum Euclidian distance from shore that will accommodate a given square window width, defined as

$$R = a\frac{\sqrt{2}}{2} \quad (1)$$

Where a is the window width associated with a single satellite pixel (for example, MERIS 300 m pixel) or a combined array of multiple satellite pixels (for example, MERIS three- by three-pixel [3 × 3-pixel] array of 300 m pixels is equal to 900 m), and R is the radius of the circle that circumscribes the pixel(s) (Fig. 3). In addition, the maximum distance to shore was calculated for each NHDPlusV2 NLA waterbody. If an NHDPlusV2 NLA waterbody's maximum distance to shore is $\geq R$, the waterbody would accommodate a window width of a. For example, using Eq. (1) a single 300 m MERIS satellite pixel has a radius R = 212 m and a 3 × 3 array of 300 m MERIS pixels has a radius R = 636 m.

2.3. Spatial coverage of public water surface intakes and potential recreational/ecological cyanoHAB exposures

The U.S. EPA Office of Ground Water and Drinking Water provided the locations of PWSIs. A PWSI was assigned to an NHDPlusV2 NLA waterbody if it was within a 100 m buffer distance and retained for further analysis. The 100 m buffer is predefined by the PWSI database and cannot be altered. PWSI locations were spatially joined to the nearest suitable satellite pixels. Isolated pixels and pixels not occurring in clusters of at least four or more (2 × 2-pixel matrix or larger) were eliminated from analysis to minimize the effect of mixed land-water boundary pixels. To determine cyanoHAB abundance for a specific PWSI, it was necessary to determine which water pixels in the satellite imagery should be linked with each PWSI. Ideally, the PWSI is within or immediately adjacent to a 3 × 3-pixel array to allow robust estimation of cyanoHAB abundance directly impacting that PWSI. A 3 × 3-pixel array was selected because satellite navigation may not be accurate to the pixel, so this area represents the water characteristics surrounding the location of utility intake. Unfortunately, few PWSIs met this criterion. PWSIs often were not directly adjacent to definable water bodies, or could be associated only with smaller water bodies lacking 3 × 3-pixel arrays. Additionally, work at all scales is useful for potential recreational and ecological exposures assessment.

To account for this variation, four categories were developed to link a PWSI with particular Areas of Interest (AOI), the group of pixels used to generate cyanoHAB abundance for the linked PWSI (Fig. 4). These categories are progressively more liberal in their assignment of water pixels to PWSI. Therefore, they offer a potential tradeoff between locational accuracy (highest with the most conservative category, #1 below) and broader coverage (highest with the most liberal category, #4 below). PWSIs that could not be associated with any pixels satisfying the first four categories also were identified. The five categories are summarized below.

- Adjacent AOI: CyanoHAB abundance was assessed for the nearest scenario using a 3 × 3-pixel satellite array centered within 300 m (one MERIS pixel) of a PWSI location. This best case scenario identified PWSIs either within or directly adjacent to an available 3 × 3-pixel satellite array, where adjacent is defined as less distant than a single 300 m pixel.
- Proximate AOI: CyanoHAB abundance was assessed for the nearest

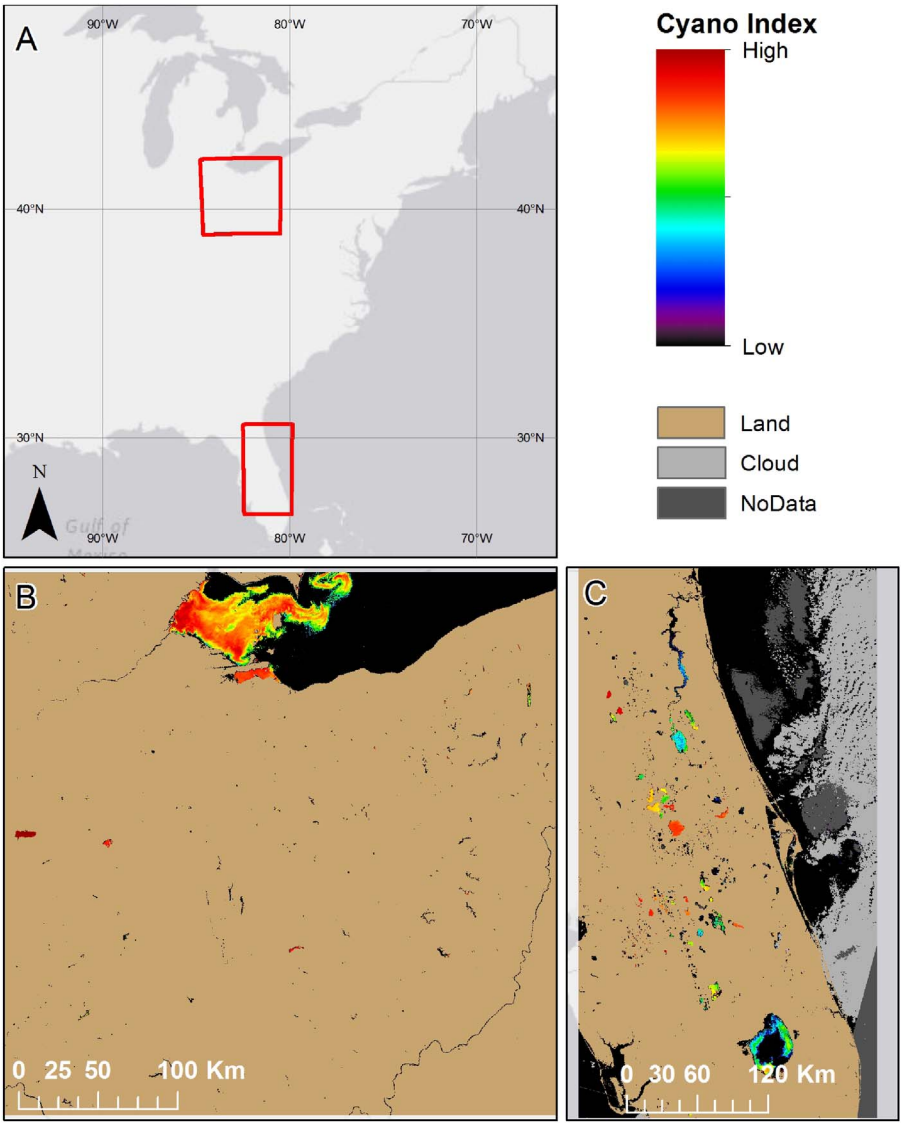

Fig. 1. Study area location map (A) indicates MERIS scene boundaries for (B) Ohio and (C) Florida. The representative single-day images for Ohio was from 9/3/2011 and for Florida was from 10/18/2010. Brown pixels are land masks; black, dark-grey, and light-grey pixels indicate a low likelihood of bloom, no data, and cloud cover respectively. Colored pixels indicate cyanoHAB abundances from high (red) to low (purple). (For interpretation of the references to colour in this figure legend, the reader is referred to the web version of this article.)

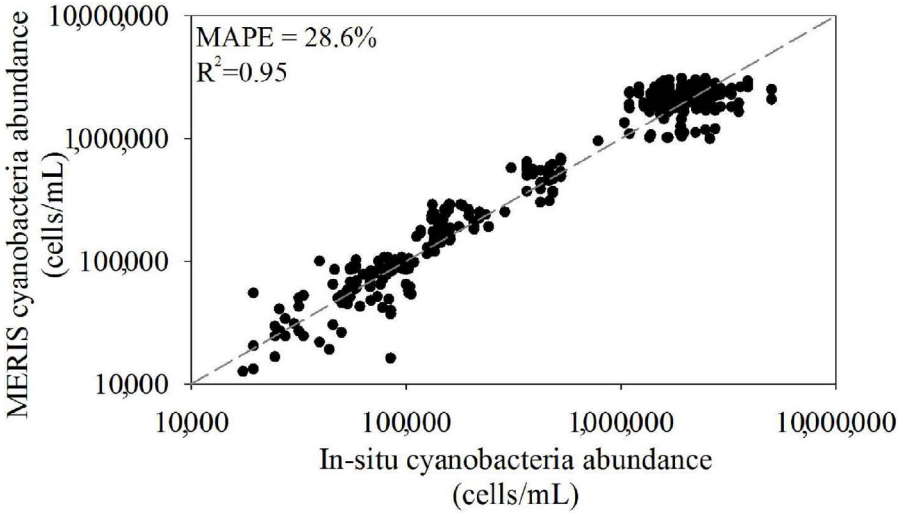

Fig. 2. Previous validation of CI algorithm using all cyanobacterial cell count available in situ data within ± 7-days of the satellite overpass from Florida, Ohio, and New England states revised from Lunetta et al. (2015). Revisions include presentation of the data in log space, mean absolute percent error (MAPE), and coefficient of determination with the exclusion of algorithm non-detects and minimum detect values.

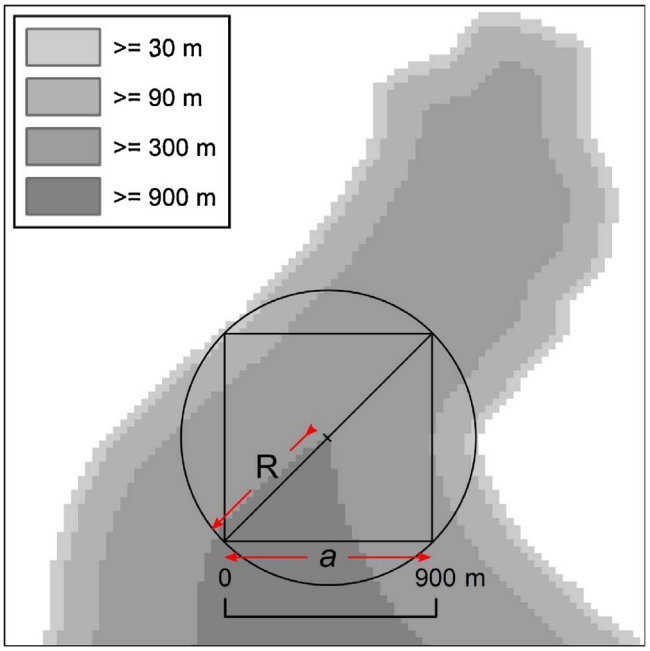

Fig. 3. This example estimation of lake, reservoir and pond satellite spatial coverage, where *a* was the window width and *R* was the radius of the circle that circumscribes the pixel(s). The example is shown for a window width of 900 m, representing a 3 × 3-pixel array of 300 m MERIS pixels. Shading indicates the maximum window width that can be accommodated as specified in the legend.

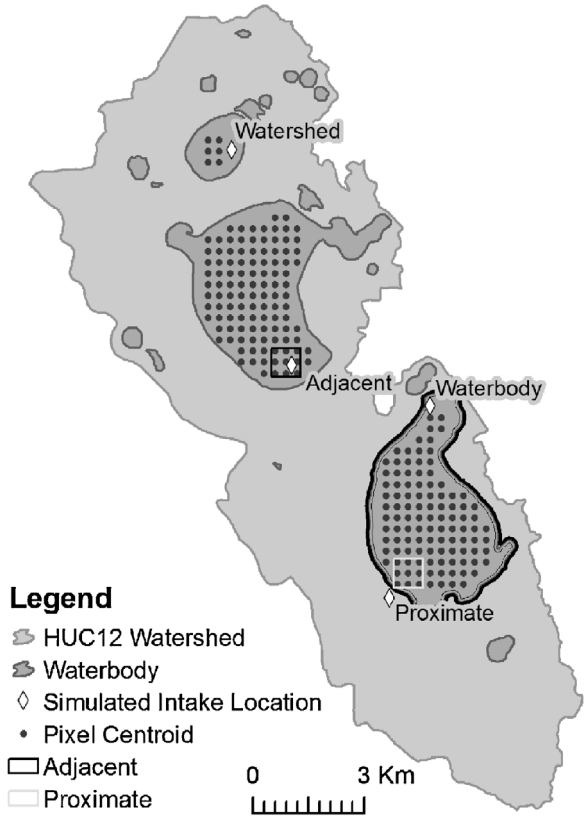

Fig. 4. Areas of interest (AOI) for resolving public surface water intakes (PWSI) using different combinations of 300 m MERIS satellite pixels. Adjacent AOIs use the nearest 3 × 3-pixel array within 300 m of the PWSI location. Proximate AOIs use the nearest 3 × 3-pixel array within 900 m of the PWSI location. Waterbody AOIs use all satellite pixels of the nearest waterbody with ≥9 pixels within 900 m of PWSI location. Watershed AOIs use all pixels within the HUC12 watershed with ≥9 pixels that encompasses the PWSI location.

3 × 3-pixel satellite array centered within 900 m of a PWSI location. The proximate AOI category is identical to the adjacent AOI category except that the maximum distance is increased to 900 m (width of a single 3 × 3-pixel array).

- Waterbody AOI: CyanoHAB abundance was assessed for all satellite pixels of the nearest waterbody with ≥9 pixels within 900 m of a PWSI location. In this case, it is assumed that a neighboring waterbody adequately represents the AOI waterbody.
- Watershed AOI: CyanoHAB abundance was assessed for all satellite pixels within the Hydrologic Unit Code (HUC) 12 watershed with ≥ 9 pixels encompassing the PWSI location. If no waterbody with sufficient available pixels can be identified within 900 m of a PWSI location, the entire watershed encompassing that PWSI was considered, assuming that the watershed has at least 9 resolvable pixels (at least as many pixels as a standard 3 × 3-pixel array).
- Unresolvable AOI: No candidate satellite pixels satisfied the criteria in categories 1 through 4.

If a PWSI fit the criteria of the adjacent AOI category, then that PWSI also was included in AOIs 2 through 4. Each PWSI subsequently was added to the next representative AOI category. For example, any proximate PWSI also fit the criteria of the waterbody and watershed AOI categories, but not the criteria of the adjacent AOI category. The waterbody and watershed AOI categories provide cyanoHAB information relevant to human and ecological health risks for evaluating exposure potential within a waterbody or across a watershed.

2.4. Temporal coverage

A binary classification was applied to year-round observations of all pixels. The classification was either a valid cyanoHAB or invalid due to clouds, land, mixed land-water, and missing data values. The frequency of valid pixels was calculated to determine the number of valid satellite observations acquired from 2008 through 2011 as the percentage of weeks with valid observations. Counts of valid observations then were summed across the 2008 through 2011 year-round time series and divided by the total number of available scenes to summarize the percent of valid observations. The 2008 through 2011time period was selected because consistent MERIS 2- to 3-day repeat visits at full resolution within the U.S. were not routinely added until after 2007 and the satellite record ended in May 2012.

2.5. Frequency of observed cyanoHABs

The frequency of observed cyanoHABs was calculated as the fraction of total pixel observations for which cyanoHAB abundance exceeded a specified threshold, specifically, WHO's high threshold of 100,000 cells mL^{-1} (WHO, 1999). This threshold was selected for demonstration purposes, and any cyanoHAB threshold level can be used for future analysis. Similar to the method of determining the temporal coverage discussed in Section 2.4, pixel values above the WHO high threshold were classified as 1, and values below the WHO threshold were classified as 0. Values were summed for each pixel and divided by the total number of valid observations (not flagged for clouds, land, mixed land-water, or no data).

For each category relating AOIs to reported PWSI locations, a distribution of cyanoHAB frequencies across all possible AOIs was generated relevant to that category. For both the adjacent and proximate AOIs, distributions were calculated across all possible combinations of 3 × 3-pixel arrays. For the waterbody AOIs the distribution was calculated across all waterbodies with ≥ 9 resolvable pixels. For the watershed AOIs, the distribution was calculated across all watersheds with ≥ 9 resolvable pixels. For each AOI, quartiles were calculated for the full distribution of bloom frequencies, with Q1 representing the lowest quartile of frequency and Q4 representing the highest, and PWSI locations then were assigned to respective quartiles.

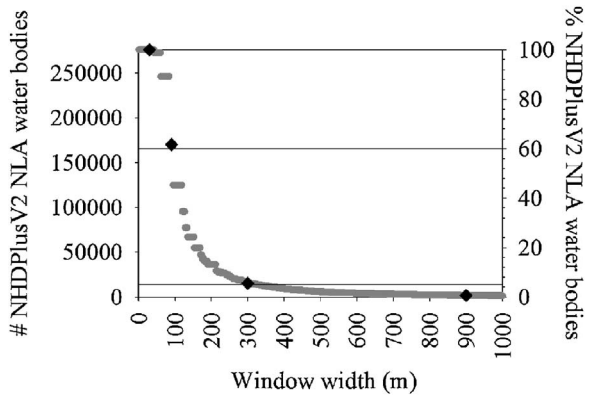

Fig. 5. Satellite spatial coverage for NHDPlusV2 NLA water bodies. Solid horizontal lines indicate that 5% and 60% of all waterbodies were resolved with 300 m and 90 m window widths, respectively. Black diamonds represent 900 m, 300 m, 90 m, and 30 m example window widths, respectively, consistent with a MERIS or Sentinel-3 Ocean and Land Colour Imager (OLCI) 900 m 3 × 3-pixel array, single 300 m pixel, and higher-resolution sensors such as the Landsat OLI and Sentinel-2 MSI 30 m pixel or 90 m 3 × 3-pixel array.

3. Results

3.1. Spatial resolution of waterbodies

Of the 379,097 lake, pond, and reservoir NHDPlusV2 waterbodies within the continental United States, 275,897 (73%) remained after the U.S. EPA NLA 2012 criteria were applied. Of these waterbodies, 5.6% were resolvable by a window width 300 m wide, a resolution equivalent to one MERIS pixel (Fig. 5). Increasing the window width to 900 m (equivalent to a 3 × 3-pixel array), reduced coverage to 0.7% of waterbodies. Any window width where $a < 42$ m resolved all waterbodies as defined by the U.S. EPA NLA 2012 criteria. Therefore, by ignoring window widths < 42 m, we were able to fit a power function regression defined as $y = 781{,}700{,}770(a)^{-1.9}$ with $R^2 = 0.99$. This function allowed interpolation of the number of resolvable water bodies at any arbitrary window width.

3.2. Spatial resolution of public water surface intakes

A total of 3086 individual PWSI locations were reported within 100 m of a valid waterbody nationally. A total of 1991 unique waterbodies were associated with at least one PWSI location. Given that a single waterbody may have multiple PWSI locations, there are more PWSI locations than unique waterbodies associated with a PWSI. Use of a window width of 300 m resolved 57% of PWSI locations and 43% of waterbodies associated with a PWSI. Increasing the window width to 900 m reduced coverage to 33% of PWSI locations and 15.1% of waterbodies associated with a PWSI. Access to higher resolution satellite imagery would substantially increase the spatial coverage of PWSI locations.

After applying the EPA NLA 2012 criteria, there were 10,910 waterbodies in Florida and 4591 waterbodies in Ohio, and 8.3% of waterbodies in Florida and 2.8% of waterbodies in Ohio were resolvable by the 300 m MERIS pixel resolution. Increasing the window width to 900 m decreased waterbody resolvability to 1.3% and 0.4% in Florida and Ohio, respectively. In Florida, 10 PWSI locations were associated with five unique waterbodies. Use of a window width of 300 m was able to resolve eight PWSI locations associated with four unique waterbodies. A 900 m window width decreased spatial coverage to seven PWSI locations associated with three waterbodies. For Ohio, 187 PWSI locations were associated with 98 waterbodies. Of these, 88 PWSI locations associated with 32 waterbodies were resolved at 300 m, and 51 PWSI locations associated with 10 waterbodies were resolvable at 900 m.

Table 1 shows the number of PWSI locations in Florida and Ohio spatially resolved by satellite under the five AOI categories. As anticipated, the least number of PWSI locations could be resolved under the adjacent AOI category. The greatest number of PWSI locations could be resolved under the waterbody AOI category. Only 10% (19) of 189 total PWSI locations were resolved using the adjacent AOI category, 22.2% (42) were resolved using the proximate AOI category, 26.4% (50) were resolved using the waterbody AOI, and 11.6% (22) using the watershed AOI. The watershed AOI yielded lower coverage than the waterbody AOI category in Ohio largely due to the effect of Lake Erie, which was associated with a large number of PWSI locations but did not fall within a watershed in this analysis. All PWSI locations in the Florida study region were spatially resolvable in at least one of the four AOI categories. In Ohio, 74.3% of the PWSI locations could not be resolved using even the most liberal watershed AOI category (AOI 4), because lakes were generally smaller in this state.

3.3. Temporal coverage

As described in Section 2.1, temporal coverage was calculated for Florida and Ohio as the percentage of weeks with valid observations across the study period. Mean temporal coverage was 80% (± 0.0003% SE) of weeks across Florida and 67% (± 0.0002% SE) across Ohio. The distribution of temporal coverage was narrow and unimodal across each region (Fig. 6) indicating lakes generally have the same amount of data coverage across each state. In Florida, 80% of pixels represented valid observations 90% of the time, and in Ohio, 70% of pixels represented valid observations 70% of the time.

3.4. Frequency of observed cyanoHABs

Fig. 7 illustrates cyanoHAB frequency as the per-pixel percentage of observed cyanobacterial abundance exceeding the WHO high threshold of 100,000 cells mL^{-1} for Florida. A pixel value of 1 indicates all observations were above the WHO threshold, and a pixel value of 0 indicates no observations above the threshold. The mean weekly cyanoHAB frequency across all pixels in Florida was 30.1%, (σ = 29.9%), and in Ohio was 4.6% (σ = 11%). The waterbodies with the highest observed bloom frequencies per region were Lake Apopka, FL (99.1%) and Grand Lake St. Marys, OH (83%).

Quartiles (Table 2) calculated for bloom frequency reveal a broad range of cyanoHAB activity across all waterbodies. Fig. 8 shows a representative time series, one for each quartile, of observations above the WHO high-threshold for four waterbody AOI locations. The fourth quartile (Q4) example in Fig. 8D indicates a higher frequency of pixels exceeding the WHO high threshold, and greater temporal persistence of high cyanoHAB abundance. Modest differences were observed between the Q1, Q2, and Q3 examples. In the most extreme case, a Q4 time series would report 100% of pixels exceeding the WHO threshold for nearly the entire time period (not shown). Seasonal patterns reflected typical bloom trends and were repeated across years with variable magnitudes. These temporal patterns suggest potential in scaling this approach for individual systems in addition to state, regional, and national applications.

Fig. 9 shows the distribution of cyanoHAB frequency across all possible AOIs relevant to each of the four categories used to associate an AOI with reported PWSI locations. AOIs were ranked by frequency of pixels over the WHO threshold, with overall frequencies ranging from 0% for the lowest rank to over 99% for the highest rank. Distributions of bloom frequency were markedly different depending on whether they were calculated based on all 3 × 3 pixel arrays (8A and 8B), waterbody (8C), or watershed (8D) AOI rankings. The upper quartile (Q4) was at 8.5% for both adjacent and proximate AOI rankings. In contrast, Q4 was 40% and 42% when distributions were determined for all waterbodies and watersheds, respectively.

The highest number of PWSI-associated AOI falling into Q4 were found using the proximate category (11 out of 42, or 26.2%; see

Table 1
Number of PWSI locations in Florida and Ohio spatially resolved by satellite under the five AOI categories.

State	PWSI AOI Category					Total PWSI Locations[a]
	Adjacent	Proximate	Waterbody	Watershed	Unresolvable	
Ohio	18	35	42	12	133	179
Florida	1	7	8	10	0	10
Sum total	*19*	*42*	*50*	*22*	*133*	*189*

[a] Total number of surface intakes for each location.

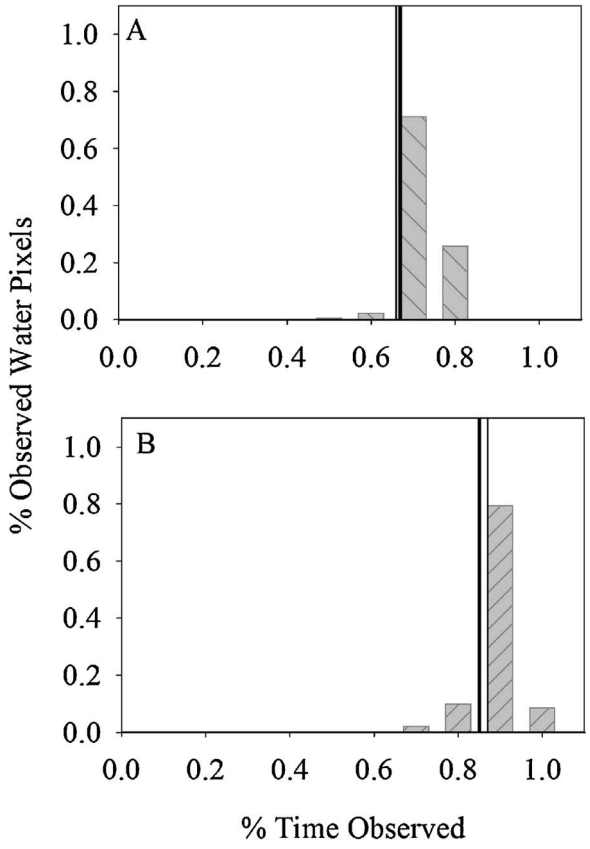

Fig. 6. Distribution for percentage of time pixels observed as cloud free and percentage of MERIS resolvable water pixels observed in (A) Ohio and (B) Florida from 2008 through 2011. The thick black line represents the mean, and the thin black line represents the median.

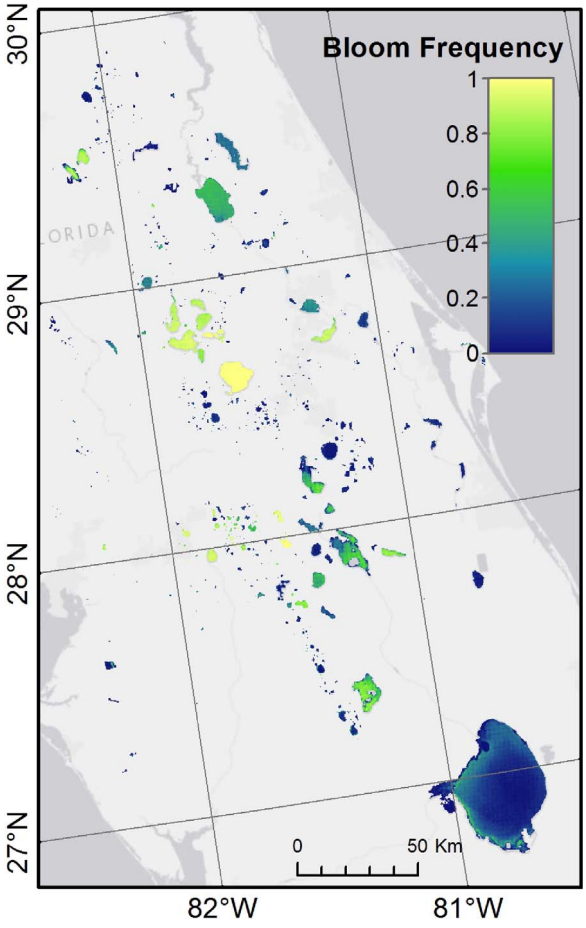

Fig. 7. Frequency of observed cyanoHAB occurrence above WHO high threshold in Florida from 2008 through 2011. A value of 1 indicates that the pixel was observed to have cyanoHABs above the WHO threshold in all observations, and a value of 0 indicates that the pixel had no cyanoHABs above the threshold.

Table 2). A similar percentage but lower number of AOIs fell into Q4 under the adjacent category (4 out of 19, or 21%). The waterbody and watershed AOI rankings resulted in dramatically lower frequencies of PWSI-associated AOIs falling into the highest quartile (2% under the waterbody criterion, 7.7% under the watershed criterion). This pattern likely reflects the effect of averaging cyanoHAB frequency over larger surface areas in these cases.

Regional differences also are apparent in the distribution of cyanoHAB frequencies. Under the adjacent AOI category, the single resolvable PWSI location in Florida fell into Q4. In Ohio, most PWSI locations fell into Q2 (11 out of 18, 61%), with only 16.7% falling into Q4. A similar but less dramatic pattern held for the proximate AOI category, with 42.9% of PWSI locations falling into Q4 in Florida, compared to only 22.8% for Ohio. Analyses under the waterbody and watershed AOI categories were less likely to place PWSI locations into the highest quartile, with no PWSI locations under either category falling into Q4 for Florida and with only 2.4% of the PWSI locations under the waterbody category and 8.3% of the PWSI locations under the watershed category falling into Q4 in Ohio.

Table 2
Quartile ranking for the adjacent, proximate, waterbody, and watershed AOI categories for Ohio and Florida PWSI bloom frequency locations.

AOI Category	State	Q1	Q2	Q3	Q4	All
Adjacent	Florida	0	0	0	1	1
	Ohio	1	11	3	3	18
Proximate	Florida	0	2	2	3	7
	Ohio	4	12	11	8	35
Waterbody	Florida	3	1	4	0	8
	Ohio	35	2	4	1	42
Watershed	Florida	3	3	4	0	10
	Ohio	1	3	7	1	12

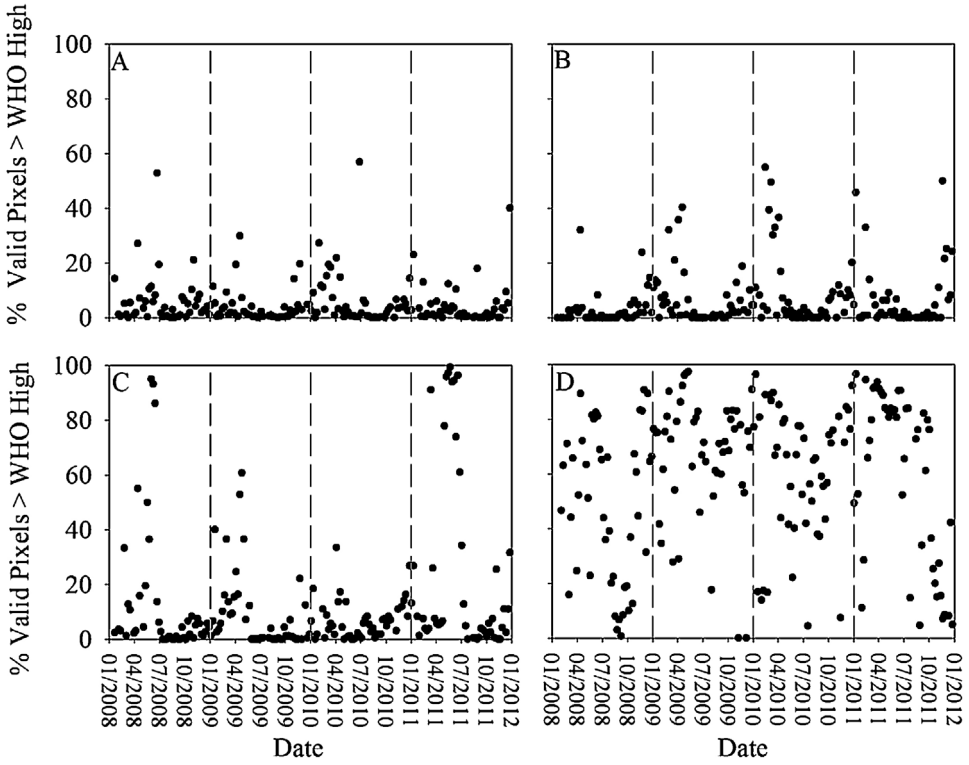

Fig. 8. Representative percent valid MERIS pixels above the WHO threshold for (A) 0–25% Q1, (B) 25–50% Q2, (C) 50–75% Q3, and (D) 75–100% Q4 using the waterbody AOI category in Florida. (A) may represent a response more similar to oligotrophic waters, and (D) may represent hypereutrophic waters. Weekly composites were used for the complete calendar years 2008 through 2011. Vertical grey dashed lines mark calendar years.

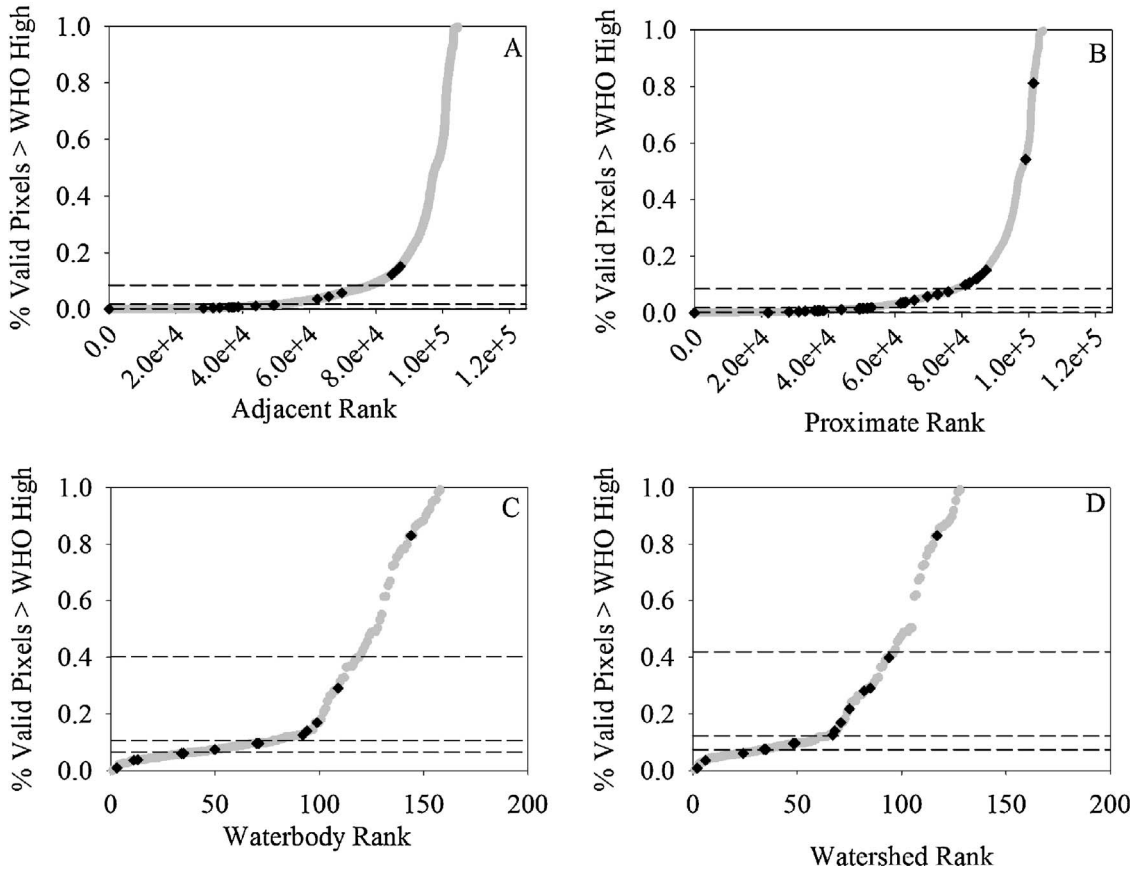

Fig. 9. Distribution of satellite derived cyanoHAB abundance valid pixels > WHO high threshold for NHDPlusV2 NLA waterbodies and PWSI locations across Ohio and Florida from 2008 through 2011. (A) Adjacent, (B) proximate, (C) waterbody, and (D) watershed AOI rankings were separated into quartiles indicated by dashed horizontal lines. Gray points represent the AOI for all resolvable locations, and black diamonds represent PWSI locations.

4. Discussion

Measures of cyanoHAB abundance have already proven useful as biological, recreational, and health indicators in many international assessment programs and organizations, such as the U.S. EPA NLA, Baltic Marine Environment Protection Commission Helsinki Commission (HELCOM), Europe's Water Framework Directive (Phillips et al., 2013), and WHO (Chorus and Cavalieri, 2000). CyanoHABs may serve as an indicator because they are easily measured from satellite, respond quickly to ecosystem alterations, may be mitigated through management actions, and are a response to anthropogenic eutrophication (Dale and Beyeler, 2001). Although this method is demonstrated using the WHO high threshold and satellite coverage for only two U.S. states, it also provides great flexibility. As mentioned in Section 2.5, any threshold may be selected, depending on stakeholder needs and requirements, such as a different jurisdictional risk thresholds. This method is also spatially and temporally scalable. Spatially, the indicator assessment could be scaled up to regions or the continent, or scaled down to a specific management district or even a single pixel. Temporally, the frequency counts could be calculated yearly or back through the historical archive of the satellite record. For example, at the federal level, there may be interest to conduct this assessment method for the entire nation, using any detectable level of cyanoHABs and the entire satellite record, to develop a national ranking of recreational waterbodies and PWSIs with the greatest exposure to cyanoHABs. However, each state could also rank only its resolved waterbodies to assist with prioritizing resources for management. Overall, policy makers and environmental managers may use cyanoHAB frequency-of-occurrence maps and rankings as early-warning indicators of areas more likely to experience blooms at the local scale while maintaining continuous national coverage, or to quantify change in cyanoHABs over time.

Although satellite based methods provide great flexibility at new spatial and temporal scales of monitoring, there are limitations. First, the MERIS archive data date back to 2002, but consistent 2- to 3-day repeat visits at full resolution within the U.S. were not routinely added until after 2007, thus restricting the study period for this analysis to 2008 through 2011. All satellite algorithms to derive geophysical variables have error associated with model performance (Schaeffer et al., 2013b), as does in situ sampling and laboratory analysis (Trees et al., 1985). Lunetta et al. (2015) report correspondence across the spectrum of cyanoHAB abundance ranges spanning 10,000 to > 1 million cells mL^{-1}. Satellite derived values below 109,000 cells mL^{-1} and above 1,000,000 cells mL^{-1} had correspondence above 80% with in situ samples collected within 7 days of a satellite overflight match up. The CI algorithm had a lower correspondence performance of 110,000 to 1,000,000 cells mL^{-1}, which was expected due to the availability of only a few in situ measures in this abundance range and the ± 7-day temporal window for coincident satellite match-ups. The binary categorization of values either above or below 100,000 cells mL^{-1}, used in this approach would further reduce the impact on algorithm error and uncertainties. In the future, validation exercises would optimally be compared with cell biovolume or pigment concentrations instead of cell counts. The biovolume impacts on reflectance are determined by the quantity of pigment and scattering of individual species, which can differ by an order of magnitude and would improve satellite validation efforts. However, taxonomic biovolume reporting is not standard and pigment measurements are rare. All satellite algorithms detect only near-surface concentrations, but the red and near-infrared part of the spectrum provide information from only the upper 1 m of the water column (Kirk, 1994). High cyanoHAB abundance near the surface poses risk during recreational activities, such as swimming and boating. Subsurface abundance of cyanoHABs also poses a risk for PWSIs. Combined information on surface blooms with physical factors like wind stress and speed will improve the inference of the vertical distribution of cyanoHABs in the future (Wynne et al., 2010). Cloud cover and ice formation limited the usability of satellite images at different rates, depending on the climatology of the studied location. As Fig. 6 shows, more cloud-free pixels were available for longer in Florida than Ohio. This discrepancy in temporal coverage likely reflects expected differences in cloud cover due to variations across latitude (Mercury et al., 2012), and also due to local impacts by large lakes in Florida, which create conditions that reduce convective cloud development, especially in summer. The frequency-of-occurrence method could suffer from bias in detection of cyanoHABs across regions with different cloud coverage, but the ability to provide synoptic coverage may outweigh this issue. Originally, this study included New England states with cloud-free pixels an average of 47% of the time. New England results were removed from this analysis after it was discovered that sensor saturation over ice caused algorithm failures during winter months and incorrectly resulted in cyanoHAB detections between November and March each year. New England could be included after an appropriate ice flag is applied to the satellite processing.

Spatial resolution remains a major limitation for monitoring inland waters due to the necessity to repurpose both current and future ocean color and land satellite sensors to answer relevant questions related to water quality science, applications, and management. Verpoorter et al. (2014) reported that waterbodies with area > 100 ha (1 square kilometer [km^2]) comprise 60% of total surface area of global inland waters, which suggests that a sensor with 300 m resolution could resolve over half of global inland waters by area. The percentage of resolved surface area is important and relevant, especially when considering factors as the global carbon cycles and continued rapid construction of dams to create reservoirs (Lehner et al., 2011; Nilsson et al., 2005). However, Hestir et al. (2015, see Fig. 4) demonstrates that the percentage of resolved surface area can vary greatly across continents due to geomorphology. Therefore, use of the total surface area of a waterbody could confuse the understanding of how many waterbodies may benefit from satellite data for decision making because of a bias toward inland waterbodies with larger surface area. For example, in the U.S., the Great Lakes alone comprise 2.44×10^7 hectares (244,079 km^2), or roughly 35% of the total freshwater surface area. Similarly, it has been estimated that data from MERIS or OLCI could provide coverage to 57% of the world's lakes with area > 100 ha (1 km^2) (Matthews et al., 2010) based on estimates from Downing et al. (2006). However, these larger waterbodies clearly are not the sole potential targets of management concern.

Results from this study suggest that previous reports of satellite coverage may indeed present a misleading estimate of the degree to which satellite imagery can resolve waterbodies. Estimates of satellite coverage in the current study (Fig. 5) indicate that < 1% of all U.S. waterbodies > 1 ha are resolvable by a 3 × 3-pixel MERIS array and that only 5.6% are resolvable by even a single MERIS pixel. These results show important constraints on management utility posed by currently available satellite resolution. Increases in resolution to levels commensurate with other satellite platforms (such as Landsat OLI and Sentinel-2 MSI) would dramatically improve coverage of smaller waterbodies and substantially increase the value of satellite imagery for assessing water quality at specific locations. In practice, the combination of satellites, in situ sondes, field sampling, and coupled modeling efforts will provide the best available information for water quality assessments because these methods all provide observations at different spatial and temporal scales.

Ideally, a PWSI will be directly under satellite pixels and far enough removed from land that only a signal from the water is measured, with no potential for mixed land-water signals. This ideal scenario was rarely the situation during this study based on the limited number of adjacent AOIs in Ohio and Florida. A number of PWSI reported locations were at the land-water interface or just downstream, directly where satellite pixels were flagged for stray-light contamination of the brightly reflected light from land. Although these PWSI locations were not directly under a useful satellite pixel, the data from the proximate AOI

still provided relevant information that could be considered representative of water characteristics surrounding that particular location because of hydrology and the amount of water a utility pulls per day. Some PWSIs were in narrower locations of a lake where enough pixels could not be resolved immediately within the 900 m buffer of the location. However, the waterbody AOI still provided information representative of the conditions throughout the entire lake that supplied the PWSI.

Finally, many PWSIs were in lakes, reservoirs, or ponds smaller than the satellite spatial resolution would allow for sufficient derivation of cyanoHAB abundance. Therefore, this study provided cyanoHAB information on the collective waterbodies in a HUC12 watershed that could be resolved. The HUC12 watershed is a local sub-watershed level that represents interconnected water systems. This watershed approach should be treated with caution until additional tests confirm that results from waterbodies within the HUC12 watershed are consistently representative of the PWSI location. The four AOI categories decreased in representativeness of actual cyanoHAB events at the PWSI, with the adjacent AOI category providing the best direct representation and the watershed AOI category the broadest representation.

Scientific literature frequently cites that HAB events are increasing, but managers are limited in their ability to determine where these events may be occurring. This method did not address duration, and extent of cyanoHABs was addressed with a different method. The 2008 through 2011 MERIS archive may be the best historical record for comparison against future events to determine change over time as a relative baseline. Caution is needed because this 4-year period is relatively short and subject to larger scale climatological forcing. For example, in 2007 and 2008 La Niña occurred, and in 2009 and 2010, El Niño occurred, switching back to a La Niña in 2010 and 2011 (NOAA, 2016). The North Atlantic Oscillation Index was predominantly in the negative phase during all 4-years.

Despite the limited 4-year duration of satellite data from 2008 through 2011, the study results may provide useful information for following years. For example, three PWSI locations in western Lake Erie were ranked in the upper quartile during this study under the adjacent AOI category. In 2013, the Carroll Township public water system identified cyanotoxins in its source and finished drinking waters. Similarly, in 2014, a Toledo public water system that pulls from Lake Erie identified concentrations of cyanotoxins in its source and finished drinking waters. Under the proximate AOI, six PWSI locations in western Lake Erie and a PWSI in Grand Lake St. Marys, Ohio's largest inland lake, ranked in the upper quartile. Grand Lake St. Marys historically is known for eutrophication and cyanoHAB events (Steffen et al., 2014). In Florida, Lake Okeechobee was identified in the upper quartile for the adjacent and proximate AOI categories. In 2016, Lake Okeechobee was reported across national news outlets as experiencing cyanoHABs (Neuhaus, 2016). Under the waterbody and watershed AOI categories, only the Grand Lake St. Marys PWSI ranked in the upper quartile. These findings suggest that when ranking PWSIs in large and heterogeneous waterbodies, it is extremely important to use the AOI closest to the intake location.

This satellite based method may provide frequency-of-occurrence information for ecological and scientific studies. It also may support national and state management needs. For example, nationally, cyanotoxins are included in the SDWA CCL and UCMR (U.S. EPA, 2013a, 2016a, 2016b). Ten cyanotoxins are included in the proposed list of 30 chemical contaminants to be sampled during the fourth UCMR event between 2018 and 2020 (U.S. EPA, 2015b). The method developed here may provide relevant source water cyanoHAB occurrence and location information to assist in the future evaluation of cyanotoxin health effects and the levels at which they occur in drinking water. Frequency-of-occurrence information may also assist with ecological health, such as the prioritization of waterbodies to develop numeric nutrient criteria (Schaeffer et al., 2013a; Schaeffer et al., 2012) or for adaptive management practices, such as green infrastructure practices or technologies. This satellite method may provide relevant ecological health information related to cyanobacterial biomass such as hypoxic events that may cause death of fauna (Paerl et al., 2001), changes in phytoplankton community composition (Dokulil and Teubner, 2000; Huisman et al., 2004), and overall reduction in photosynthetic light availability due to bloom shading (Tilzer, 1987). States also may use this information to assist with prioritizing limited resources to address recreational waters or PWSIs with the greatest frequency of occurrence. The method may provide states with information on previously unsampled lakes. The scientific research community may benefit by targeting additional scientific studies on topics such as land management or human health effects related to cyanoHABs. Overall, this method may improve general awareness about and preparedness for cyanoHABs for resolvable public water system utilities, especially smaller utilities that serve < 10,000 people. The method developed here to identify resolvable surface water bodies for cyanoHAB remote sensing analysis can be extended to other sensors (such as Landsat or MODIS) and other water quality parameters (such as chlorophyll-a, turbidity, and temperature). Additionally, the method used to associate PWSI point locations with remotely sensed water quality data could be extended to examine the relationship between gridded water quality data and other point locations of interest, such as release locations.

5. Conclusions

This study identified a number of resolvable U.S. inland water bodies based on calculations using different window width resolutions to demonstrate the potential applicability of information from satellite sensors about water quality related to cyanoHABs. Ocean color imagers traditionally are limited in spatial resolution for inland aquatic applications, including the Copernicus program new series of Sentinel-3 OLCIs (Berger et al., 2012; Donlon et al., 2012) at 300 m that replaced the previous MERIS sensor on the Envisat satellite. A 300 m resolution sensor may provide data for 15,545 (5.6%) continental U.S. NLA lakes and reservoirs, if it is optimistically assumed that the resolution at nadir is the same at the edge of the swath. A conservative 3 × 3-pixel grid may provide data for 1862 (< 1%) of U.S. NLA lakes and reservoirs. Single 300 m pixel resolution resolved 57% of PWSIs and a 3 × 3-pixel array resolved 33% of PWSIs. Land imagers such as the Landsat OLI and Copernicus program Sentinel-2 MSI sensors have a higher spatial resolution of 30 m but less frequent revisit cycles and less available wavebands for deriving water quality parameters (for example, they cannot directly measure phycocyanin to differentiate cyanobacteria from phytoplankton). The Copernicus program is a 15+ year monitoring program that includes the Sentinel-3 and Sentinel-2 series satellites (Berger et al., 2012). At the time of writing (2017), Sentinel-3A and Sentinel-2A were already in orbit and providing data. Identical Sentinel–3 B and Sentinel–2 B satellites were nearing readiness for launch, and with two identical satellites in orbit repeat times will be reduced and temporal coverage of inland waters increased. Therefore, future land imagers must be considered as part of the comprehensive management toolbox for monitoring water quality. A 30 m resolution sensor may provide data for 275,897 (100%) U.S. lakes and reservoirs at single pixel resolution or 170,240 (62%) lakes and reservoirs using a 3 × 3-pixel grid. A single Landsat OLI 30 m pixel resolution resolved 100% of PWSIs and a 3 × 3-pixel array resolved 95% of PWSIs.

The study results demonstrate a relatively straight forward approach to assess the frequency of cyanoHAB occurrence by calculating the number of observed values above a selected threshold divided by the total number of observations. Four methods of calculating cyanoHAB occurrence at PWSI locations were identified. Spatial maps of the frequency of events over time permit easy identification of locations prone to cyanoHAB exposures in recreational and drinking source waterbodies. These same maps may allow managers to create national or regional rankings of cyanoHAB occurrence to quantify and help prioritize locations in the upper quartiles that may require more

immediate attention and adaptive management solutions. This study is the first of its kind to compare occurrence of cyanoHABs across multiple locations both for recreational and drinking source waterbodies. The demonstration of these new satellite based methods may assist in the development of management objectives and contribute as part of a more comprehensive management approach.

Acknowledgements

This work was supported by the NASA Ocean Biology and Biogeochemistry Program/Applied Sciences Program (proposal 14-SMDUNSOL14- 0001), the NASA Applied Sciences/Public Health and Water Quality Program (NNH08ZDA001N), and by U.S. EPA, NOAA, and the U.S. Geological Survey Toxic Substances Hydrology Program. This article has been reviewed by the National Exposure Research Laboratory and Office of Water and approved for publication. Mention of trade names or commercial products does not constitute endorsement or recommendation for use by the U.S. Government. The views expressed in this article are those of the authors and do not necessarily reflect the views or policies of the U.S. EPA. We acknowledge Jacobs Laboratory Support Team for providing technical edits, and thank the anonymous reviewers for their comments and suggestions.

References

Al-Tebrineh, J., Merrick, C., Ryan, D., Humpage, A., Bowling, L., Neilana, B.A., 2012. Community composition, toxigenicity, and environmental conditions during a cyanobacterial bloom occurring along 1,100 kilometers of the Murray River. Appl. Environ. Microbiol. 78, 263–272.

Backer, L.C., McNeel, S.V., Barber, T., Kirkpatrick, B., Williams, C., Irvin, M., Zhou, Y., Johnson, T.B., Nierenberg, K., Aubel, M., LePrell, R., Chapman, A., Foss, A., Corum, S., Hill, V.R., Kieszak, S.M., Cheng, Y.-S., 2010. Recreational exposure to microcystins during algal blooms in two California lakes. Toxicon 55, 909–921.

Backer, L.C., Landsberg, J.H., Miller, M., Keel, K., Taylor, T.K., 2013. Canine cyanotoxin poisonings in the United States (1920s-2012): review of suspected and confirmed cases from three data sources. Toxins 5, 1597–1628.

Backer, L.C., Manassaram-Baptiste, D., LePrell, R., Bolton, B., 2015. Cyanobacteria and algae blooms: review of health and environmental data from the harmful algal bloom related illness surveillance system (HABISS) 2007–2011. Toxins 7, 1048–1064.

Baith, K., Lindsay, R., Fu, G., McClain, C.R., 2001. SeaDAS: Data analysis system developed for ocean color satellite sensors. EOS, Transactions. Am. Geophys. Union 82, 202.

Berger, M., Moreno, J., Johannessen, J.A., Levelt, P.F., Hanssen, R.F., 2012. ESA's sentinel missions in support of Earth system science. Remote Sens. Environ. 120, 84–90.

Carroll, M.L., Townshend, J.R., DiMiceli, C.M., Noojipady, P., Sohlberg, R.A., 2009. A new global raster water mask at 250 m resolution. Int. J. Digital Earth 2, 291–308.

Chorus, I., Cavalieri, M., 2000. Cyanobacteria and algae. In: Bartram, J., Rees, G. (Eds.), Monitoring Bathing Waters—A Practical Guide to the Design and Implementation of Assessments and Monitoring Programmes. World Health Organization, London.

Chorus, I.E., 2012. Current Approaches to Cyanotoxin Risk Assessment, Risk Management and Regulations in Different Countries. Federal Environment Agency (Umweltbundesamt).

Codd, G.A., Lindsay, J., Young, F.M., Morrison, L.F., Metcalf, J.S., 2005a. Harmful cyanobacteria: from mass mortalities to management measures. In: Huisman, J., Matthijs, H.C.P., Visser, P.M. (Eds.), Harmful Cyanobacteria. Springer, Netherlands, pp. 1–23.

Codd, G.A., Morrison, L.F., Metcalf, J.S., 2005b. Cyanobacterial toxins: risk management for health protection. Toxicol. Appl. Pharmacol. 203, 264–272.

Dale, V.H., Beyeler, S.C., 2001. Challenges in the development and use of ecological indicators. Ecol. Indic. 1, 3–10.

Dodd, S.R., Haynie, R.S., Williams, S.M., Wlide, S.B., 2016. Alternate food-chain transfer of the toxin linked to avian vacuolar myelinopathy and implications for the endangered Florida snail kite (Rostrhamus sociabilis). J. Wildl. Dis. 52, 335–344.

Dodds, W.K., Bouska, W.W., Eitzmann, J.L., Pilger, T.J., Pitts, K.L., Riley, A.J., Schloesser, J.T., Thornbrugh, D.J., 2009. Eutrophication of U.S. freshwaters: analysis of potential economic damages. Environ. Sci. Technol. 43, 12–19.

Dokulil, M.T., Teubner, K., 2000. Cyanobacterial dominance in lakes. Hydrobiologia 438, 1–12.

Donlon, C., Berruti, B., Buongiorno, A., Ferreira, M.-H., Féménias, P., Frerick, J., Goryl, P., Klein, U., Laur, H., Mavrocordatos, C., Nieke, J., Rebhan, H., Seitz, B., Stroede, J., Sciarra, R., 2012. The global monitoring for environment and security (GMES) Sentinel-3 mission. Remote Sens. Environ. 120, 37–57.

Dörnhöfer, K., Oppelt, N., 2016. Remote sensing for lake research and monitoring −recent advances. Ecol. Indic. 64, 105–122.

Dörra, F.A., Pintoa, E., Soaresb, R.M., Azevedo, S.M.F.d.O.e., 2010. Microcystins in South American aquatic ecosystems: occurrence, toxicity and toxicological assays. Toxicon 56, 1247–1256.

Downing, J.A., Prairie, Y.T., Cole, J.J., Duarte, C.M., Tranvik, L.J., Striegl, R.G., McDowell, W.H., Kortelainen, P., Caraco, N.F., Melack, J.M., Middelburg, J.J., 2006. The global abundance and size distribution of lakes, ponds, and impoundments. Limnol. Oceanogr. 51, 2388–2397.

Duan, H., Ma, R., Xu, X., Kong, F., Hao, J., Shang, L., 2009. Two-decade reconstruction of algal blooms in China's Lake Taihu. Environ. Sci. Technol. 43, 3522–3528.

Falconer, I.R., Humpage, A.R., 2005. Health risk assessment of cyanobacterial (blue-green algal) toxins in drinking water. Int. J. Environ. Res. Public Health 2, 43–50.

Falconer, I.R., 1999. An overview of problems caused by toxic blue?green algae (cyanobacteria) in drinking and recreational water. Environ. Toxicol. 14, 5–12.

Graham, J.L., Loftin, K.A., Kamman, N., 2009. Monitoring Recreational Freshwaters. North American Lake Management Society, Lakeline Summer, pp. 18–24.

Harke, M.J., Steffen, M.M., Gobler, C.J., Otten, T.G., Wilhelm, S.W., Wood, S.A., Paerl, H.W., 2016. A review of the global ecology, genomics, and biogeography of the toxic cyanobacterium, Microcystis spp. Harmful Algae 54, 4–20.

Henry, T., 2013. Toxins Overwhelm Carroll Township Water Plant. The Blade, Toledo OH.

Hestir, E.L., Brando, V.E., Bresciani, M., Giardino, C., Matta, E., Villa, P., Dekker, A.G., 2015. Measuring freshwater aquatic ecosystems: the need for a hyperspectral global mapping satellite mission. Remote Sens. Environ. 167, 181–195.

Hilborn, E.D., Beasley, V.R., 2015. One health and cyanobacteria in freshwater systems: animal illnesses and deaths are sentinel events for human health risks. Toxins 7, 1374–1395.

Hilborn, E.D., Roberts, V.A., Backer, L., DeConno, E., Egan, J.S., Hyde, J.B., Nicholas, D.C., Wiegert, E.J., Billing, L.M., DiOrio, M., Mohr, M.C., Hardy, F.J., Wade, T.J., Yoder, J.S., Hlavsa, M.C., 2014. Algal bloom associated disease outbreaks among users of freshwater lakes—United States, 2009–2010. Morb. Mortal. Wkly. Rep. 63, 11–15.

Hitzfeld, B.C., Lampert, C.S., Spaeth, N., Mountfort, D., Kaspar, H., Dietrich, D.R., 2000. Toxin production in cyanobacterial mats from ponds on the McMurdo Ice Shelf, Antarctica. Toxicon 38, 1731–1748.

Hoeger, S.J., Hitzfeld, B.C., Dietrich, D.R., 2005. Occurrence and elimination of cyanobacterial toxins in drinking water treatment plants. Toxicol. Appl. Pharmacol. 203, 231–242.

Huisman, J., Sharples, J., Stroom, J.M., Visser, P.M., Kardinaal, W.E.A., Verspagen, J.M.H., Sommeijer, B., 2004. Changes in turbulent mixing shift competition for light between phytoplankton species. Ecology 85, 2960–2970.

Kahru, M., Savchuk, O.P., Elmgren, R., 2007. Satellite measurements of cyanobacterial bloom frequency in the Baltic Sea: interannual and spatial variability. Mar. Ecol. Prog. Ser. 343, 15–23.

Kirk, J.T.O., 1994. Light and Photosynthesis in Aquatic Ecosystems. Cambridge University Press, New York.

Kutser, T., 2009. Passive optical remote sensing of cyanobacteria and other intense phytoplankton blooms in coastal and inland waters. Int. J. Remote Sens. 30.

Lehner, B., Liermann, C.R., Revenga, C., Vorosmarty, C., Fekete, B., Crouzet, P., Doll, P., Endejan, M., Frenken, K., Magome, J., Nilsson, C., Robertson, J.C., Rodel, R., Sindorf, N., Wisser, D., 2011. High-resolution mapping of the world's reservoirs and dams for sustainable river-flow management. Front. Ecol. Environ. 9, 494–502.

Lévesque, B., Gervais, M.C., Chevalier, P., Gauvin, D., Anassour-Laouan-Sidi, E., Gingras, S., Fortin, N., Brisson, G., Greer, C., Bird, D., 2014. Prospective study of acute health effects in relation to exposure to cyanobacteria. Sci. Total Environ. 466–467, 397–403.

Lévesque, B., Gervais, M.C., Chevalier, P., Gauvin, D., Anassour-Laouan-Sidi, E., Gingras, S., Fortin, N., Brisson, G., Greer, C., Bird, D., 2016. Exposure to cyanobacteria: acute health effects associated with endotoxins. Public Health 134, 98–101.

Lin, C.J., Wade, T.J., Sams, E.A., Dufour, A.P., Chapman, A.D., Hilborn, E.D., 2016. A prospective study of marine phytoplankton and reported illness among recreational beachgoers in Puerto Rico, 2009. Environ. Health Perspect. 124, 477–483.

Loftin, K.A., Graham, J.L., Hilborn, E.D., Lehmann, S.C., Meyer, M.T., Dietze, J.E., Griffith, C.B., 2016. Cyanotoxins in inland lakes of the United States: occurrence and potential recreational health risks in the EPA national lakes assessment 2007. Harmful Algae 56, 77–90.

Lunetta, R.S., Shao, Y., Ediriwickrema, J., Lyon, J.G., 2010. Monitoring agricultural cropping patterns across the Laurentian Great Lakes Basin using MODIS-NDVI data. Int. J. Appl. Earth Obs. Geoinf. 12, 81–88.

Lunetta, R.S., Schaeffer, B.A., Stumpf, R.P., Keith, D., Jacobs, S.A., Murphy, M.S., 2015. Evaluation of cyanobacteria cell count detection derived from MERIS imagery across the eastern USA. Remote Sens. Environ. 157, 24–34.

Matthews, M.W., Bernard, S., Winter, K., 2010. Remote sensing of cyanobacteria-dominant algal blooms and water quality parameters in Zeekoevlei, a small hypertrophic lake, using MERIS. Remote Sens. Environ. 114, 2070–2087.

McKay, L., Bondelid, T., Dewald, T., Johnston, J., Moore, R., Rea, A., 2012. NHDPlus Version2: User Guide.

Medina-Cobo, M., Domínguez, J.A., Quesada, A., Hoyos, C.d., 2014. Estimation of cyanobacteria biovolume in water reservoirs by MERIS sensor. Water Res. 63, 10–20.

Mercury, M., Green, R., Hook, S., Oaida, B., Wu, W., Gunderson, A., Chodas, M., 2012. Global cloud cover for assessment of optical satellite observation opportunities: a HyspIRI case study. Remote Sens. Environ. 126, 62–71.

Meriluoto, J., Spoof, L., Codd, G.A., 2017. Handbook of Cyanobacterial Monitioring and Cyanotoxin Analysis. John Wiley Sons, Ltd.

Michalak, A.M., Anderson, E.J., Beletsky, D., Boland, S., Bosch, N.S., Bridgeman, T.B., Chaffin, J.D., Cho, K., Confesor, R., Daloglu, I., DePinto, J.V., Evans, M.A., Fahnenstiel, G.L., He, L., Ho, J.C., Jenkins, L., Johengen, T.H., Kuo, K.C., LaPorte, E., Liu, X., McWilliams, M.R., Moore, M.R., Posselt, D.J., Richards, R.P., Scavia, D., Steiner, A.L., Verhamme, E., Wright, D.M., Zagorski, M.A., 2013. Record-setting algal bloom in Lake Erie caused by agricultural and meteorological trends consistent with expected future conditions. Proc. Natl. Acad. Sci. U. S. A. 110, 6448–6452.

Mouw, C.B., Greb, S., Aurin, D., DiGiacomo, P.M., Lee, Z., Twardowski, M., Binding, C.,

Hu, C., Ma, R., Moore, T., Moses, W., Craig, S.E., 2015. Aquatic color radiometry remote sensing of coastal and inland waters: challenges and recommendations for future satellite missions. Remote Sens. Environ. 160, 15–30.
NOAA, 1950. Historical El Nino/La Nina Episodes (1950s-Present). National Weather Service Climate Prediction Center. http://www.cpc.noaa.gov/products/analysis_monitoring/ensostuff/ensoyears.shtml.
Neuhaus, L., 2016. Reeking, Oozing Algae Closes South Florida Beaches. New York Times. http://www.nytimes.com/2016/07/02/us/reeking-oozing-algae-closes-south-florida-beaches.html?_r=2.
Nilsson, C., Reidy, C.A., Dynesius, M., Revenga, C., 2005. Fragmentation and flow regulation of the world's large river systems. Science 308, 405–408.
Paerl, H.W., Huisman, J., 2008. Blooms like it hot. Science 320, 57–58.
Paerl, H.W., Fulton, R.S., Moisander, P.H., Dyble, J., 2001. Harmful freshwater algal blooms, with an emphasis on cyanobacteria. Sci. World 1 76-13.
Palmer, S.C.J., Kutser, T., Hunter, P.D., 2015. Remote sensing of inland waters: challenges, progress and future directions. Remote Sens. Environ. 157, 1–8.
Phillips, G., Lyche-Solheim, A., Skjelbred, B., Mischke, U., Drakare, S., Free, G., Järvinen, M., Hoyos, C.D., Morabito, G., Poikane, S., Carvalho, L., 2013. A phytoplankton trophic index to assess the status of lakes for the water framework directive. Hydrobiologia 704, 75–95.
Pilotto, L.S., Douglas, R.M., Burch, M.D., Cameron, S., Beers, M., Rouch, G.J., Robinson, P., Kirk, M., Cowie, C.T., Hardiman, S., Moore, C., Attewell, R.G., 1997. Health effects of exposure to cyanobacteria (blue-green algae) during recreational water-related activities. Aust. N. Z. J. Public Health 21, 562–566.
Qin, B., Zhu, G., Gao, G., Zhang, Y., Li, W., Paerl, H.W., Carmichael, W.W., 2010. A drinking water crisis in Lake Taihu, China: linkage to climatic variability and lake management. Environ. Manage. 45, 105–112.
Schaeffer, B.A., Hagy, J.D., Conmy, R.N., Lehrter, J.C., Stumpf, R.P., 2012. An approach to developing numeric water quality criteria for coastal waters using the SeaWiFS satellite data record. Environ. Sci. Technol. 46, 916–922.
Schaeffer, B., Hagy, J.D., Stumpf, R.P., 2013a. An approach to developing numeric water quality criteria for coastal waters: a transitiion from SeaWiFS to MODIS and MERIS satellites. J. Appl. Remote Sens. 7, 073544.
Schaeffer, B.A., Schaeffer, K.G., Keith, D., Lunetta, R.S., Conmy, R., Gould, R.W., 2013b. Barriers to adopting satellite remote sensing for water quality management. Int. J. Remote Sens. 34, 7534–7544.
Smayda, T.J., 1997. What is a bloom? A commentary. Limnol. Oceanogr. 42, 1132–1136.
Song, K., Li, L., Li, Z., Tedesco, L., Hall, B., Shi, K., 2013. Remote detection of cyanobacteria through phycocyanin for water supply source using three-band model. Ecol. Inf. 15, 22–33.
Song, K., Li, L., Tedesco, L.P., Li, S., Hall, B.E., Du, J., 2014. Remote quantification of phycocyanin in potable water sources through an adaptive model. ISPRS J. Photogramm. Remote Sens. 95, 68–80.
Sonich-Mullin, C., 2014. Keeping an eye on harmful algal blooms., EPA Science in Action.
Steffen, M.M., Zhu, Z., McKay, R.M.L., Wilhelm, S.W., Bullerjahn, G.S., 2014. Taxonomic assessment of a toxic cyanobacteria shift in hypereutrophic Grand Lake St. Marys (Ohio, USA). Harmful Algae 33, 12–18.
Steffensen, D.A., 2008. Economic cost of cyanobacterial blooms. In: Hudnell, H.K. (Ed.), Cyanobacterial Harmful Algal Blooms: State of the Science and Research Needs. Springer, New York, pp. 855–865.
Stewart, I., Robertson, I.M., Webb, P.M., Schluter, P.J., Shaw, G.R., 2006a. Cutaneous hypersensitivity reactions to freshwater cyanobacteria–human volunteer studies. BMC Dermatol. 6.
Stewart, I., Webb, P.M., Schluter, P.J., Fleming, L.E., Burns, J.W., Gantar, M., Backer, L.C., Shaw, G.R., 2006b. Epidemiology of recreational exposure to freshwater cyanobacteria −an international prospective cohort study. BMC Public Health 6.
Stumpf, R.P., Wynne, T.T., Baker, D.B., Fahnenstiel, G.L., 2012. Interannual variability of cyanobacterial blooms in Lake Erie. PLoS One 7, e42444.
Stumpf, R.P., Davis, T.W., Wynne, T.T., Graham, J.L., Loftin, K.A., Johengen, T.H., Gossiaux, D., Palladino, D., Burtner, A., 2016. Challenges for mapping cyanotoxin patterns from remote sensing of cyanobacteria. Harmful Algae 54, 160–173.
Tilzer, M.M., 1987. Light-dependence of photosynthesis and growth in cyanobacteria: implications for their dominance in eutrophic lakes. N. Z. J. Mar. Freshwater Res. 21, 401–412.
Tomlinson, M.C., Stumpf, R.P., Wynne, T.T., Dupuy, D., Burks, R., Hendrickson, J., Fulton, R.S., 2016. Relating chlorophyll from cyanobacteria-dominated inland waters to a MERIS bloom index. Remote Sens. Lett. 7, 141–149.
Trees, C.C., Kennicut, M.C., Brooks, J.M., 1985. Errors associated with the standard fluorimetric determination of chlorophylls and phaeopigments. Mar. Chem. 17, 1–12.
Tyler, A.N., Hunter, P.D., Spyrakos, E., Groom, S., Constantinescu, A.M., Kitchen, J., 2016. Developments in Earth observation for the assessment andmonitoring of inland, transitional, coastal and shelf-sea waters. Sci. Total Environ. http://dx.doi.org/10.1016/j.scitotenv.2016.01.020.
USEPA, 2011. 2012 National Lakes Assessment Site Evaluation Guidelines. Office of Water, Washington, DC EPA 841-B-11-005.
U.S. EPA, 2013a. CCL and Regulatory Determinations: CCL 3 List. http://water.epa.gov/scitech/drinkingwater/dws/ccl/index.cfm
USEPA, 2013b. The Importance of Water to the U.S. Economy: Synthesis Report. Office of Water, Washington, DC (p. 29.).
USEPA, 2014. Cyanobacteria and Cyanotoxins: Information for Drinking Water Systems. Office of Water, Washington, DC (EPA −810F11001).
USEPA, 2015a. Drinking Water Health Advisory for the Cyanobacterial Microcystin Toxins. Office of Water, Washington, DC (p. 67., EPA-820R15100).
USEPA, 2015b. Revisions to the unregulated contaminant monitoring rule (UCMR4) for public water systems and announcement of a public meeting. Federal Register 80 76897–76923.
U.S. EPA, 2016a. CCL and Regulatory Determinations: CCL 4 List. https://www.epa.gov/ccl/draft-contaminant-candidate-list-4-ccl-4
U.S. EPA, 2016b. Fourth Unregulated Contaminant Monitoring Rule. https://www.epa.gov/dwucmr/fourth-unregulated-contaminant-monitoring-rule.
Ueno, Y., Nagata, S., Tsutsumi, T., Hasegawa, A., Watanabe, M.F., Park, H., Chen, G., Chen, G., Yus, S., 1996. Detection of microcystins, a blue-green algal hepatotoxin, in drinking water sampled in Haimen and Fusui, endemic areas of primary liver cancer in China, by highly sensitive immunoassay. Carcinogenesis 17, 1317–1321.
Verpoorter, C., Kutser, T., Seekell, D., Tranvik, L.J., 2014. A global inventory of lakes based on high-resolution satellite imagery. Geophys. Res. Lett. 41, 6396–6402.
Verschuren, D., Johnson, T.C., Kling, H.J., Edgington, D.N., Leavitt, P.R., Brown, E.T., Talbot, M.R., Hecky, R.E., 2002. History and timing of human impact on Lake Victoria, East Africa. Proc. R. Soc. Lond. B: Biol. Sci. 269, 289–294.
WHO, 1999. Toxic Cyanobacteria in Water: A Guide to Their Public Health Consequences, Monitoring and Management. E & FN Spon, New York.
Wynne, T.T., Stumpf, R.P., Tomlinson, M.C., Warner, R.A., Tester, P.A., Dyble, J., Fahnensteil, G.L., 2008. Relating spectral shape to cyanobacterial blooms in the Laurentian Great Lakes. Int. J. Remote Sens. 29, 3665–3672.
Wynne, T.T., Stumpf, R.P., Tomlinson, M.C., Dyble, J., 2010. Characterizing a cyanobacterial bloom in western Lake Erie using satellite imagery and meteorological data. Limnol. Oceanogr. 55, 2025–2036.